Laminar flame characteristics of cyclopentanone at elevated temperatures

Bao, X., Jiang, Y., Xu, H., Wang, C., Lattimore, T. & Tang, L.

Author post-print (accepted) deposited by Coventry University's Repository

Original citation & hyperlink:

Bao, X, Jiang, Y, Xu, H, Wang, C, Lattimore, T & Tang, L 2017, 'Laminar flame characteristics of cyclopentanone at elevated temperatures' Applied Energy, vol 195, pp. 671-680.
https://dx.doi.org/10.1016/j.apenergy.2017.03.031

DOI 10.1016/j.apenergy.2017.03.031
ESSN 0306-2619
Publisher: Elsevier

NOTICE: this is the author's version of a work that was accepted for publication in *Applied Energy*. Changes resulting from the publishing process, such as peer review, editing, corrections, structural formatting, and other quality control mechanisms may not be reflected in this document. Changes may have been made to this work since it was submitted for publication. A definitive version was subsequently published in *Applied Energy*, Vol 195, (2017) DOI: 10.1016/j.apenergy.2017.03.031

© 2017, Elsevier. Licensed under the Creative Commons Attribution-NonCommercial-NoDerivatives 4.0 International
http://creativecommons.org/licenses/by-nc-nd/4.0/

Copyright © and Moral Rights are retained by the author(s) and/ or other copyright owners. A copy can be downloaded for personal non-commercial research or study, without prior permission or charge. This item cannot be reproduced or quoted extensively from without first obtaining permission in writing from the copyright holder(s). The content must not be changed in any way or sold commercially in any format or medium without the formal permission of the copyright holders.

This document is the author's post-print version, incorporating any revisions agreed during the peer-review process. Some differences between the published version and this version may remain and you are advised to consult the published version if you wish to cite from it.

Laminar Flame Characteristics of Cyclopentanone at Elevated Temperatures

Xiuchao Bao [a, b] , Yizhou Jiang [c, b], Hongming Xu [a, b, c*], Chongming Wang[b], Thomas Lattimore [b], Lan Tang [a]
[a] School of Automobile and Transportation, Xihua University, Chengdu, China
[b] University of Birmingham, Birmingham, UK
[c] State Key Laboratory of Automotive Safety and Energy, Tsinghua University, Beijing, China

Abstract: Cyclopentanone, a product of biomass pyrolysis of agricultural waste, has certain advantages as a biofuel candidate but so far little is known about its combustion characteristics. In this paper, the laminar flame characteristics of cyclopentanone, including stretched flame propagation speed, unstretched flame propagation speed, and laminar burning velocity, were measured and compared with gasoline and ethanol, using the outwardly propagating spherical flame method and the high-speed Schlieren photography technique. The experiments were conducted in a constant-volume vessel using various fuel-air equivalence ratios (ϕ=0.8-1.6) at elevated initial temperatures (T_0=423, 448 and 473 K) and a fixed initial pressure (P_0=0.1 MPa). Linear and non-linear extrapolations were used to characterise the relationship between the stretch rate and the stretched flame propagation speed when Markstein length was near to or away from zero respectively. Empirical functions were obtained to calculate the laminar burning velocities of cyclopentanone for various fuel-air equivalence ratios and initial temperatures.The results show that Markstein length of cyclopentanone decreases when equivalence ratio is increased, and the turning point of equivalence ratio at which it changes from positive to negative is slightly below1.4. The maximum laminar burning velocity of cyclopentanone appears at the equivalence ratio of approximately 1.2, regardless of the initial temperature. The laminar burning velocity of cyclopentanone has a smaller difference to that of ethanol and gasoline when equivalence ratio is leaner than stoichiometric, but when equivalence ratio increases from1.0 to 1.4, it becomes increasingly lower than that of ethanol and higher than that of gasoline. The maximum laminar burning velocity of cyclopentanone is 0.82 m/s; for gasoline it is 0.72 m/s and for ethanol it is 0.86 m/s, at an initial temperature of 423 K and pressure of 0.1MPa.

Keywords: Cyclopentanone; Laminar burning velocity; Markstein length; Constant-volume vessel

Nomenclature

ϕ	Fuel-air equivalence ratio	
S_n	Stretched flame propagation speed	m/s
S_l	Unstretched flame propagation speed	m/s
u_l	Laminar burning velocity	m/s
α	Stretch rate	1/ms
r	Instantaneous flame radius	mm
L_b	Markstein length	mm
ρ_b	Density of burned gas	kg/m^3
ρ_u	Density of unburned gas	kg/m^3
α_T	Temperature exponent	
T_0	Initial temperature	K
P_0	Initial pressure	MPa
t	Time	ms

1. Introduction

Using biofuels is widely regarded as one the most desirable solutions to meet the dual challenges of environmental protection and energy security [1-2]. A promising generation of biofuels is characterized by a rich source of raw materials, fast renewable speed, potential to reduce greenhouse gas emissions, and promotion of agricultural economic development [3-5]. Currently, ethanol is one of the main renewable liquid fuels produced on a large scale in parallel with biodiesel. However, ethanol suffers from several limitations, such as low energy density and high energy consumption during its production. Recently, significant progress in manufacturing new biofuels has been made by using a new catalytic biomass-to-liquid process to convert both fructose and glucose to the furan series family of molecules [6-7]. Among these molecules is cyclopentanone, a product of biomass pyrolysis of agricultural waste into furfural, which is then converted to cyclic ketone by aqueous hydrogenation[8-12].

Cyclopentanone is a colourless liquid with low toxicity, and has similar specific properties to gasoline and ethanol, shown in Table 1. It is oxygenated with an oxygen content of 19.05% and it has an H/C ratio of 1.6. Cyclopentanone has a volumetric density of 0.9487 g/cm^3, much higher than that of gasoline and ethanol. The heat of vaporization of cyclopentanone is higher than that of gasoline, which is an advantage in increasing air intake charge thus power density in internal combustion engines because the higher heat of vaporization lowers the intake charge temperature [13], especially in direct injection engines. The stoichiometric air-fuel ratio of cyclopentanone is lower than gasoline and similar to ethanol, which can lead to higher engine power-density. Cyclopentanone has an auto-ignition temperature of 445˚C, much higher than that of gasoline, indicating its excellent potential for resistance to engine knocking in spark-ignition engines, if used in gasoline blends for improving fuel economy.

Table 1 Properties of cyclopentanone [13-17]

Parameters	**Cyclopentanone**	**Gasoline**	**Ethanol**
H/C ratio	1.6	1.795	3
Density (kg/m^3)	948.7	744.5	789.0
Boiling point (K)	404	293-473	351
Auto-ignition point (K)	718	553	636
Gravimetric oxygen content (%)	19.05	0	34.78
Stoichiometric air/fuel ratio	10.6	14.6	9
LHV (MJ/kg)	34.8	44.0	26.9
Heat of vaporization (MJ/kg)	0.433	0.373	0.912
Lower limit of explosion	1.6%	1.2%	3.3%
Upper limit of explosion	10.8%	7.1%	19.0%

The combustion characteristics of the intended fuel are key inputs required by an engine designer, and this is particularly pertinent for new biofuel candidates. Laminar flame characteristics are critical in determining the combustion flame development process [2, 4, 13]. Inherent in the chemical properties of a fuel, laminar burning velocity and Markstein length are the key parameters used in the study of laminar combustion [1, 13]. Laminar burning velocity is used to verify the chemical reaction mechanism of the fuel, and it is also one of the required input parameters in the simulation of turbulent premixed flame propagation [18], as well as the simulation of the combustion process and emissions [19].

Techniques for the measurement of laminar burning velocity include using a Bunsen burner, the plane flame method, the stagnation surface method and using constant volume combustion vessels with high speed imaging. Due to the large errors associated with the Bunsen burner method, and the inconsistency in using the plane flame method, the stagnation surface and constant volume combustion methods are the ideal methods for laminar combustion measurement [20-23]. However, since the stagnation surface method cannot be used under high pressure conditions, this leaves using constant volume combustion bombs as the most widely used method to study the laminar combustion characteristics for a wide range of applications [24], as the measurement of the flame can be taken under various controlled initial conditions, including elevated temperatures. The authors' group has used this technique in the measurement of laminar burning velocity of different fuel blends [25-29], and the same technique has also been used in the study of hydrogen combustion characteristics by the first author [30-31]. The limitation of this method is that the stretched flame speed must be corrected and converted to the upstretched burning velocities, whereas the raw data obtained from the stagnation flame can be modelled readily [24].

Although the combustion characteristics of several furans as biofuel candidates, including 2, 5-dymethylfuran and 2-methylfuran, have been reported [25-27, 29], the existing literature on cyclopentanone is focused only on its production technology [32]. The laminar burning velocity of cyclopentanone is unknown, thus it is impossible for the engine community to predict the performance of the engine combustion using it as fuel [32]. In order to provide such data for the first time, this paper studies laminar combustion characteristics of cyclopentanone at different equivalence ratios (0.8-1.6) and temperatures (423-473K), benchmarked to gasoline and ethanol. The experimental investigation, using a constant volume vessel and high-speed Schlieren imaging system, aims to measure and compare the laminar burning velocity and Markstein number of cyclopentanone with gasoline and ethanol under elevated temperature conditions. The elevated initial temperatures are used to ensure cyclopentanone is fully vaporised and also closer to engine charge temperature. By using a range of different temperatures, temperature exponential factors for the combustion velocity fitting correlations at varied conditions can be obtained The experimental system and data processing techniques are described in the next section, followed by the results and discussion. The findings and conclusions of the work are given at the end of the paper.

2. Experimental system and data processing

2.1 Experimental system

Figure 1 shows a schematic of the experimental setup. It primarily consisted of the spherical constant-volume combustion vessel, fuelling system, gas exchange (intake and exhaust) system, ignition system, control and data acquisition system and high-speed Schlieren photography system.

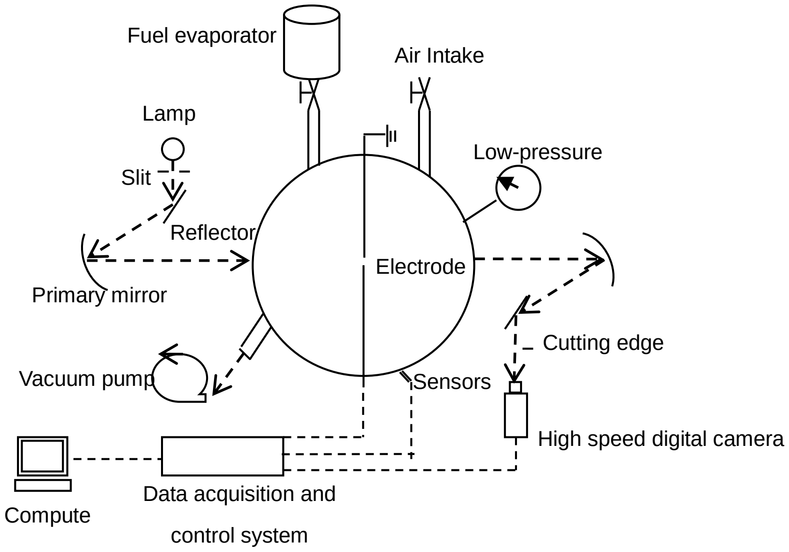

Figure 1 Schematic of the experimental setup for laminar flame measurement

The spherical constant-volume combustion vessel had an inner diameter of 350 mm, and the designed upper pressure and temperature limits were 4 MPa and 600 K, respectively. The air intake supplied from standard air bottles was introduced into the combustion vessel and heated by resistance heating coils installed in the vessel wall, and the vessel temperature could be precisely controlled by a proportional-integral-derivative (PID) controller. The combustion vessel was well wrapped by thermal insulation, reducing the heat exchange between the combustion vessel and test cell. Two opposing circular windows with effective optical diameters of 120 mm each were available for the purpose of optical access. Two opposing electrodes with a diameter of 2 mm were used as a spark plug. The ignition system also consisted of an ignition coil and a control module. The discharge energy could be adjusted by varying the TTL (transistor–transistor logic) control signal width. The exhaust gas was released thorough an exhaust valve and the vessel was vacuumed before the next test by using an air pump.

A high performance Halogen lamp was selected as the light source, which was focused onto a pinhole using a set of lenses, for the purpose of generating a spotlight for the Schlieren imaging method. Passing through a set of mirrors, the light path was then cut by the edge of a knife, which was essential for achieving the Schlieren imaging method. A Phantom V7.3 high-speed camera was used to capture the Schlieren images at a speed of 10,000 frames per second, with a resolution of 480x480 pixels. The camera was synchronized with the ignition system.

The partial pressures of fuels under various fuel-air equivalence ratios were calculated [30, 31]. Based on the calculated partial pressures, a high precision pressure transducer with an accuracy of 5×10^{-5} MPa was used to control the fuel and air quantities introduced into the combustion vessel. In this study, the initial temperature of the combustion vessel was set at 423, 448 and 473K for three different values, well above the boiling point of cyclopentanone, in order to ensure all the fuel in the vessel is vaporised.

Before each experiment, the chamber was initially vacuumed by a pump in order to remove residual gases and moisture until the pressure reached less than 0.005 MPa. Next, the fuelling valve was opened and the vaporized fuel from the fuel evaporator was introduced into the vessel. The fuel evaporator was employed to ensure all fuel was vaporized before entering the vessel and it was also important to ensure homogeneity of the fuel-air mixture in the vessel. After this step, the air was introduced into the combustion vessel through a valve. The initial pressure in the chamber was maintained at 0.1 MPa, and the temperature was controlled and maintained at a certain value for approximately 5 minutes. The fuel-air mixture was then ignited with a signal which was also used to trigger the high-speed camera and data acquisition system. After one experiment was finished, the exhaust and intake valves were both opened, and the system was purged with fresh air. The combustion vessel was then vacuumed, as the gas temperature dropped quickly to ensure it was ready for the next test.

2.2 Data processing

For quantitative analysis of laminar flame combustion, identification of the flame radius is essential. However, the flame front is not a perfect sphere, making it difficult to directly determine the flame radius. In this study, the total area enclosed by the flame front was calculated by a LabVIEW code, from which the radius was calculated. Figure 2a shows the raw flame image, and Figure 2b shows the flame front calculated by the LabVIEW code.

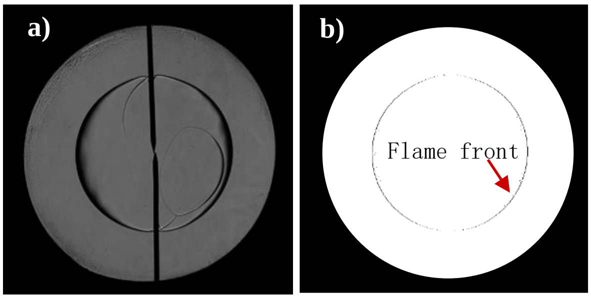

Figure 2 Flame images in the constant volume vessel : (a) Raw image; (b) Calculated flame front

Because the inner diameter of the combustion vessel was 350 mm, the burning volume fraction was less than 1/125 when the flame radius was less than 35mm, during which there was hardly any pressure changes noticeable [30, 31]. In this study, the flame images used for the measurement had flame radii between 12 mm and 28 mm. The minimum radius was selected to avoid the effect of spark ignition and the maximum radius was selected to surely meet the condition of constant pressure. The flame volume at the radius of 28 mm was only about 0.4% of the vessel, and considering the density ratio across the flame front, the mass fraction burned was even less, without causing a pressure rise as confirmed by the pressure monitoring during the test.

Parameters, including stretched flame propagation speed, unstretched flame propagation speed, laminar burning velocity, and Markstein lengths, were calculated to quantitatively describe the laminar flame characteristics. The following are the definitions of these parameters.

The stretched flame propagation speed (S_n) was calculated using the following equation:

$$S_{\mathrm{n}} = dr / dt \qquad (1)$$

where r is the flame radius and t is the time elapsed after the ignition.

For the outward propagated flame, with a known stretched flame propagation speed and radius, the stretch rate (α) can be determined using the following equation [33]:

$$\alpha = 2S_{\mathrm{n}} / r \qquad (2)$$

During the early stage of flame propagation, the relationship between the stretch rate and the stretched flame propagation speed is defined as linear in [34-35] but as non-linear in [36-37]. The linear relationship between the stretch rate and stretched flame propagation speed can be expressed as [34-35]:

$$S_{\mathrm{n}} = S_{\mathrm{l}} - L_b \alpha \qquad (3)$$

where S_l is the unstretched flame propagation speed; L_b is the Markstein length. S_l is determined by extrapolating S_n to the zero stretch rate and L_b is the negative value of the slope of the stretched flame propagation speed versus the stretch rate.

The non-linear relationship between the stretch rate and the stretched flame propagation speed can be expressed using two methods. The first non-linear relationship method is used in [36]:

$$S_{\mathrm{n}} = S_{\mathrm{l}} - 2S_{\mathrm{l}} L_{\mathrm{b}} / r \qquad (4)$$

By combining Equations 3 and 4, the following equation can be used to represent the non-linear relationship between the stretch rate and stretched flame propagation speed:

$$S_{\mathrm{n}} = S_{\mathrm{n}}{}^2 / S_{\mathrm{l}} + \alpha L_{\mathrm{b}} \qquad (5)$$

The second non-linear relationship method is used in [37]:

$$\ln(S_{\mathrm{n}}) = \ln(S_{\mathrm{l}}) - 2S_{\mathrm{l}} L_{\mathrm{b}} / (r S_{\mathrm{n}}) \qquad (6)$$

By combining the Equations 3 and 6, the stretch rate is calculated by:

$$\ln(S_{\mathrm{n}}) = \ln(S_{\mathrm{l}}) - S_{\mathrm{l}} L_{\mathrm{b}} \alpha / (S_{\mathrm{n}}{}^2) \qquad (7)$$

In reference [38], it is demonstrated that the first non-linear relationship (Equations 4-5) is the most accurate for mixtures with a positive Markstein length, while the second non-linear relationship (Equations 6-7) is the most accurate for mixtures with a negative Markstein length. However, when the Markstein length is near to zero, shown in Figure 3a, the correlation between the fitting curve and data is very poor, using either of the two non-linear methods. The results seem to indicate that in some test conditions where L_b is close or equal to zero, the linear method is suitable and works well because the fitting curve becomes linear anyway [28, 29]. In the work of Shen et al [39] and Wu et al [40] the unstretched flame propagation speed was determined through the nonlinear extrapolation method (for Le < 1) and linear extrapolation method (for Le > 1). In the present work，these three methods above have been jointly used. Before the final production of the results for the calculated flame speed, the Markstein length for each group of the data was calculated. Next, the first non-linear relationship (Equation 4-5) was used for the measurements with positive Markstein lengths (an example is the lines when ϕ <=1.2 in Figure 3b, and the second non-linear relationship (Equation 6-7) was used for negative Markstein lengths (an example is the line when ϕ =1.6 in Figure 3b. The linear method was used for Markstein lengths near to or equal to zero (an example is the line when ϕ =1.4 in Figure 3b.

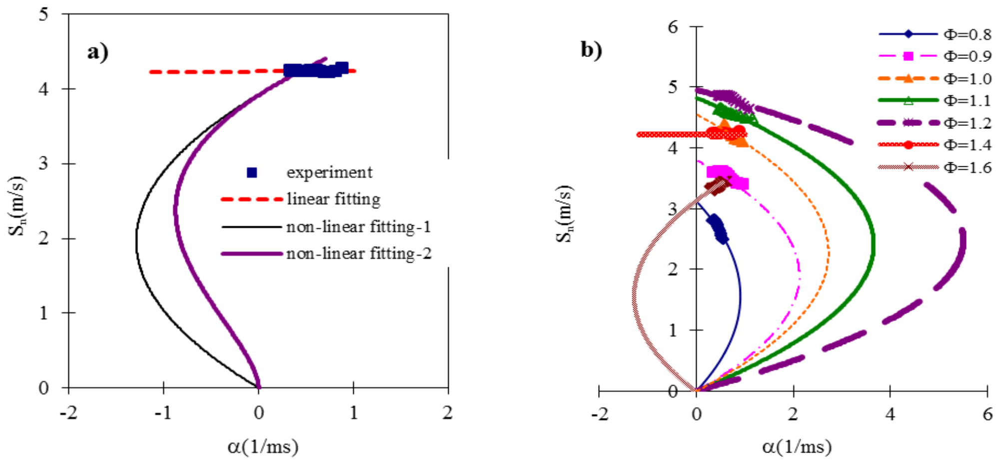

Figure 3 Relationships between stretched burning velocity and stretch rate (initial condition: T_0=423K and P_0=0.1MPa)

(a) Markstein length near to zero; (b) Markstein length under all equivalence ratios

The laminar burning velocity (u_l) can be obtained from the following equation [35]:

$$u_l = S_l \rho_b / \rho_u \qquad (8)$$

where ρ_b and ρ_u are the burned and unburned mixture densities, respectively. Assuming the pressure is constant, the burned (ρ_b) and unburned gas densities (ρ_u) can be calculated using Gaseq software [41].

It must be noted that apart from the most widely used methods for calculating laminar burning velocity using the linear and non-linear curve fittings for correcting the stretched flame speed measurement [24,29,35,41], Eisazadeh-Far et al developed a thermodynamic model based on the pressure rise during the flame propagation in constant volume vessels, taking the energy losses due to the electrodes and the vessel wall and radiation into account, as well as the temperature gradient in the preheat zone under a number of other assumptions [42, 43]. The advantages and disadvantages of the various methods for laminar burning velocity measurement have been reviewed by Ref [24].

Figure 4 presents the laminar burning velocity of ethanol available in the literature compared with that obtained in this study. The present data at 423K is close to that of Eglfopoulos [44] at 428K and the two measurements show a reasonable agreement. This approves that the method used in this study can produce reasonably reliable results within acceptable accuracy.

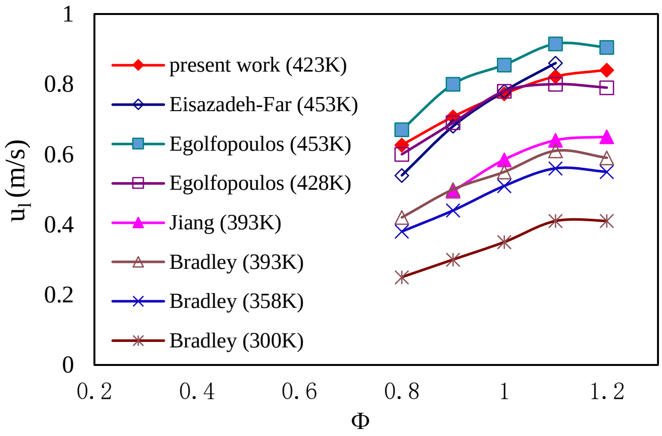

Figure 4 Laminar burning velocity of ethanol at 0.1 MP at different initial temperatures [44-46]

3. Results and discussion

3.1 Schlieren images

Figure 5 shows the Schlieren images of premixed flame propagation in cyclopentanone-air mixtures at various equivalence ratios (initial condition: T_0=423K and P_0=0.1MPa). The flame propagated faster when the fuel-air mixture was richer, and it reached its maximum flame speed at the fuel-air equivalence ratio (ϕ) of 1.2. Further increasing ϕ from 1.2 to 1.6 led to a decrease of flame speed. Compared with the rich mixtures, the initial flame speed of lean mixtures was more sensitive to changes in the equivalence ratio. Lean mixtures had a longer flame initiation (ignition delay) time [13] and the flame kernel growth rate for the equivalence ratio of 0.8 was very slow, and this caused the difference in the flame size given in Figure 6. It can be seen that the flame radius *r* increased with time *t* and the maximum flame radius acceleration occurred at the equivalence ratio of 1.2, while the minimum occurred at the smallest equivalence ratio of 0.8 (the leanest equivalence ratio tested in this study).

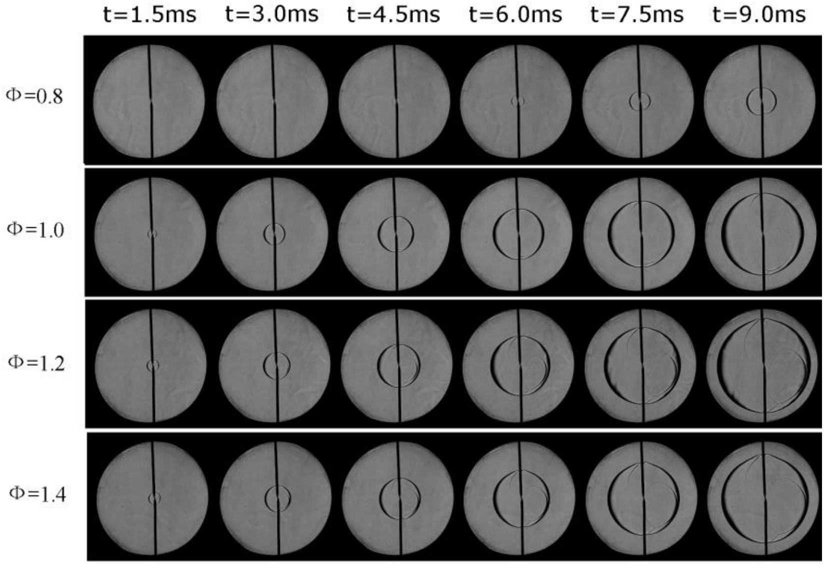

Figure 5 Schlieren images for the premixed cyclopentanone-air mixtures using various fuel-air equivalence ratios (Initial condition: T_0=423K and P_0=0.1MPa)

Figure 6 shows that the flame development delay (defined as the time for the flame radius to reach 2mm) varied with equivalence ratio. At ϕ=0.8, the flame development delay was the longest at about 4.5 ms. From the Schlieren images, there was not any detectable flame kernel before 4.5 ms at ϕ=0.8. When ϕ was increased from 0.8 to 0.9, the flame development delay was significantly decreased from about 4.5 to approximately 1.0 ms. When ϕ was further increased from 0.9 to 1.6, the flame development delay was much less sensitive to this parameter. This is because when the fuel-air mixture is very lean, the heat released near the spark electrodes is low, and part of the heat is transferred to the spark electrodes, resulting in reduced flame temperature [13]. Therefore, the flame kernel development is suppressed, leading to a longer flame development time. When fuel-air mixture is rich, the heat release rate in the flame kernel development is much higher than the heat losses and thus it is less affected by the spark electrodes [47].

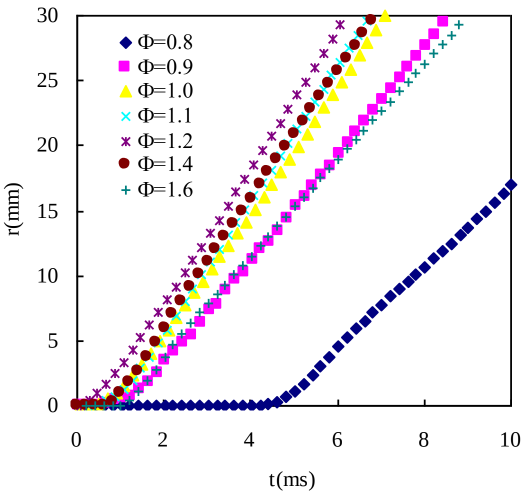

Figure 6 Flame radius changes with time for the premixed cyclopentanone-air mixtures using various fuel-air equivalence ratios (initial condition: T_0=423K and P_0=0.1MPa)

Figure 7 compares the Schlieren images for the three fuels at the equivalence ratios of 1.2 (T_0=423K and P_0=0.1MPa). It is easy to see that ethanol had the highest flame speed, gasoline had the lowest, and cyclopentanone was in the middle.

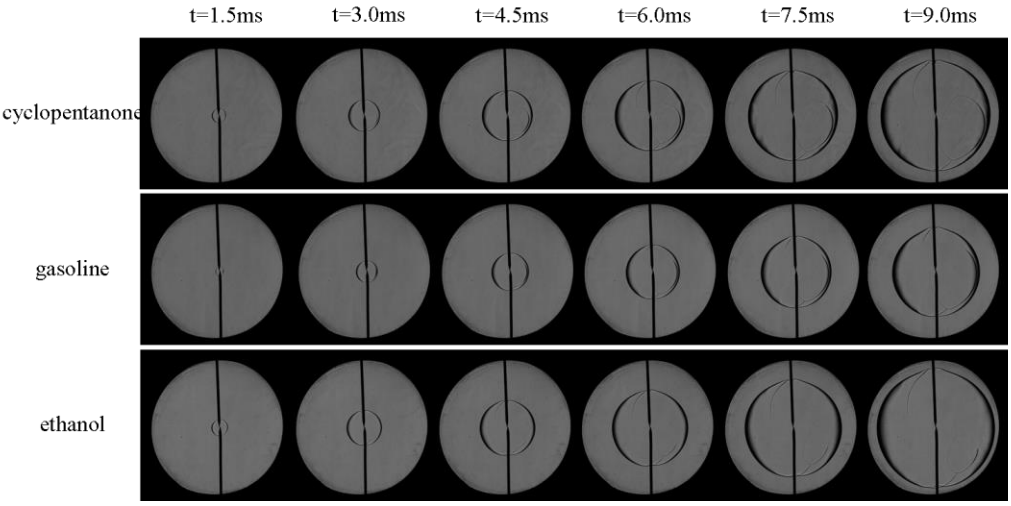

Figure 7 Schlieren images for the three fuels (Initial condition: ϕ=1.2 T_0=423K, P_0=0.1MPa)

3.2 Flame propagation speed and Markstein length

The combustion of premixed fuel-air mixtures is subject to the impact of ignition energy at the early flame development, and consequently, the flame is not stable when the flame radius is smaller than 6-8mm [20-21]. Figure

8 shows the stretched flame propagation speed for the premixed cyclopentanone-air mixtures calculated from the flame images at various equivalence ratios (initial condition: T0=423K and P0=0.1MPa). As shown in the figure, when the flame radius exceeded 12 mm, the impact of the ignition had almost diminished. However, the flame speed was affected again when combustion pressure in the constant volume vessel started to increase. The stretched flame propagation speed increased as ϕ increased from 0.8 to 1.2, and then it decreased as ϕ increased. Compared with the mixture at ϕ=0.8, the stretched flame propagation speed at ϕ=1.2 was almost twice as much fast.

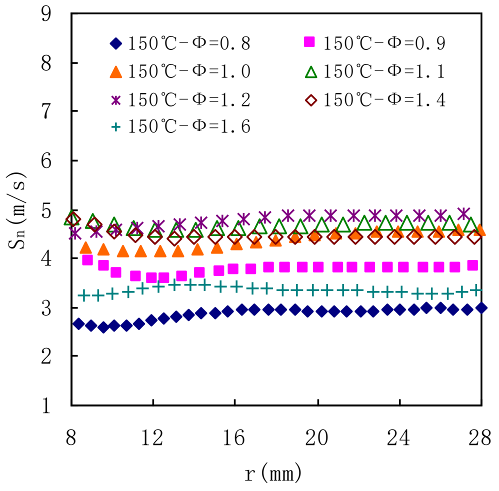

Figure 8 Stretched flame propagation speed for the premixed cyclopentanone-air mixtures using various fuel-air equivalence ratios (initial condition: T_0=423K and P_0=0.1MPa)

Figure 9a shows the Markstein lengths for the premixed cyclopentanone-air mixtures using various equivalence ratios (initial condition: T_0=423-473K and P_0=0.1MPa). Markstein length indicates the effect of stretch rate on flame propagation speed. For heavy hydrocarbon–air mixtures (molecular weight is greater than air), Markstein length decreases when equivalence ratio is increased; while for light hydrocarbon–air mixtures (molecular weight is less than air), it increases when equivalence ratio is increased [33]. The observation from Figure 6 is in agreement with this theory, since cyclopentanone is a heavy hydrocarbon fuel. It can be concluded that the diffusion-thermal instability of cyclopentanone reduces as equivalence ratio is increased.

When Markstein length is positive, the decrease of stretch rate leads to an increased unstretched flame propagation speed. When Markstein length is negative, the decrease of stretch rate leads to a reduced unstretched flame propagation speed [48]. The stretch rate always decreases with the increase of flame radius. From Figure 9a, it can be seen that the Markstein length of cyclopentanone laminar flame did not appear to change with initial temperature.However, it was highly sensitive to the fuel-air equivalence ratio. The turning point of equivalence ratio at which it changes from positive to negative is slightly below1.4. Similar trend was found in earlier study as well [49].

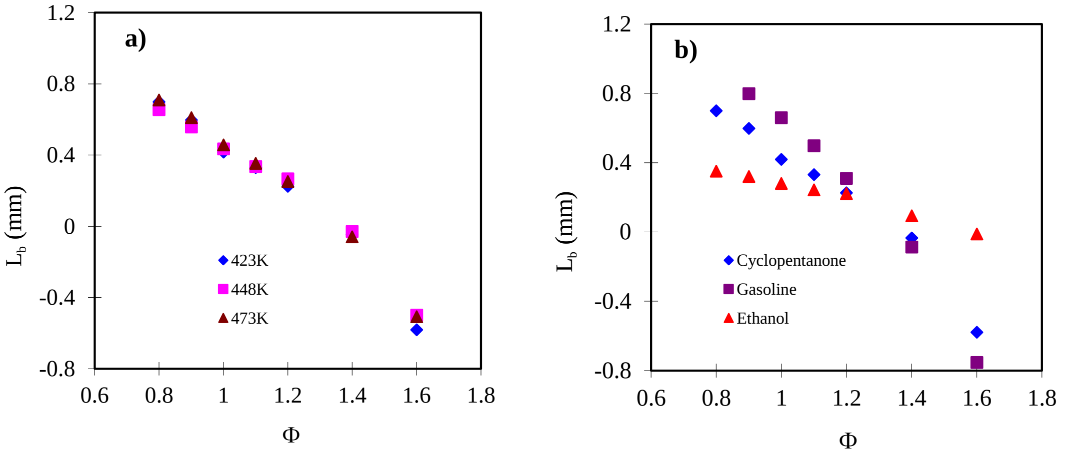

Figure 9 Markstein length using various fuel-air equivalence ratios (initial condition: P_0=0.1MPa) (a) cyclopentanone for various temperature; (b) cyclopentanone, gasoline, and ethanol for T_0=423K

From Figure 9b, it can be seen that Markstein length changed with different fuels. The Markstein lengths of these three fuels all decreased when equivalence ratio was increased, for which gasoline had the biggest slope, ethanol had the smallest, and cyclopentanone was in the middle. This shows that for lean mixtures, the stability of gasoline is the strongest and the stability of ethanol is the weakest. For rich mixtures, the stability of ethanol is the strongest, and the stability of gasoline is the weakest.

The results of the unstretched flame propagation speed is shown in Figure 10a. Increasing the initial temperature consistently resulted in a higher unstretched flame propagation speed for ϕ>=0.9. The maximum unstretched flame propagation speed was achieved at ϕ=1.2, regardless of the initial temperature. Any deviation from this optimized equivalence ratio led to a reduced unstretched flame propagation speed. However, for ϕ=0.8, the unstretched flame propagation speed changed very little for different temperatures.

Figure 10b shows the unstretched flame propagation speed of the three fuels at an initial pressure of 0.1MP and an initial temperature of 423K. It can be seen that the unstretched flame propagation speed changed with different fuels. Ethanol had the highest flame speed, gasoline had the lowest, and the cyclopentanone was in the middle. However, the different fuels had different equivalence ratios corresponding to the peak flame speed: for gasoline it was between 1.1 to 1.2, for cyclopentanone it was approximately 1.2, and for ethanol it was between 1.2 to 1.3. In leaner mixtures, the differences in unstretched flame propagation speed for the three different fuels was smaller, but, in the richer mixtures, the differences were larger, especially for $\phi >= 1.0$.

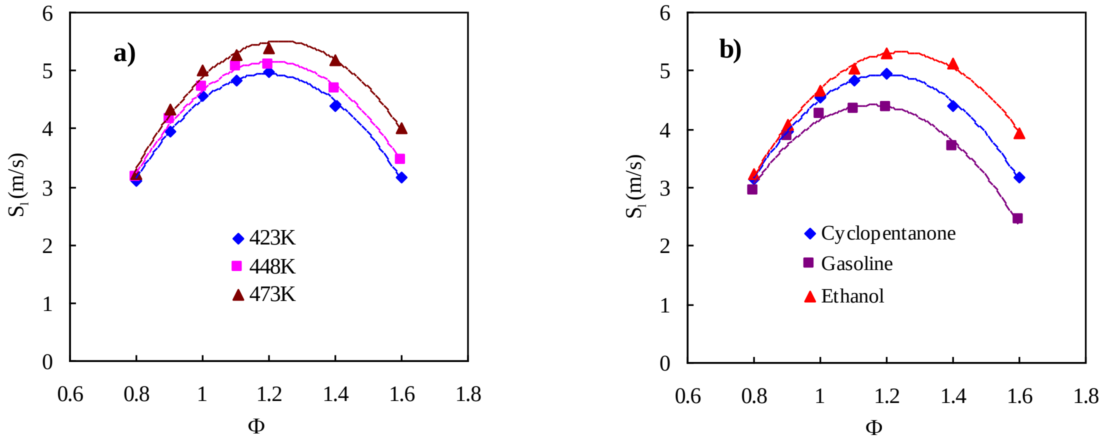

Figure 10 Unstretched flame propagation speed using various fuel-air equivalence ratios (initial condition: P_0=0.1 MPa) (a) cyclopentanone for various temperature; (b) cyclopentanone, gasoline, and ethanol for T_0=423K

3.3 Laminar burning velocity

Figure 11a presents the laminar burning velocities of premixed cyclopentanone-air mixtures using various equivalence ratios (initial conditions: T_0=423-473K and P_0= 0.1MPa). The trend of the laminar burning velocity was similar to that of the unstretched flame propagation speed, as shown in Figure 10a; when the equivalence ratio was increased, the laminar burning velocity increased at first, and then reached the maximum at ϕ=1.2. After exceeding the optimized equivalence ratio, the unstretched laminar burning velocity started to decrease. Comparing Figure 11a with Figure 10a, it can also be seen that the impact of initial temperature on the laminar burning velocity was more significant than its impact on the unstretched flame propagation speed, especially for the lean fuel-air mixtures. It is expected that the higher heat of vaporization of cyclopentanone which can result in lower intake temperature in engines (as described in the introduction) will have some offsetting effect on the laminar burning velocity thus flame speed of cyclopentanone-air mixtures in the engine cylinder.

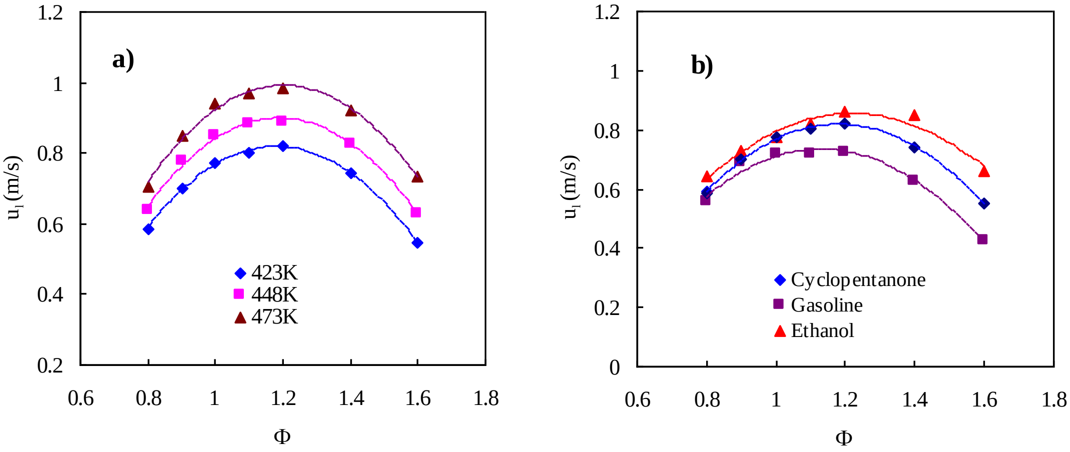

Figure 11 Laminar burning velocities using various fuel-air equivalence ratios (initial condition: P_0= 0.1MPa)
(a) cyclopentanone for various temperature; (b) cyclopentanone gasoline, and ethanol for T_0=423K

Figure 11b shows the comparison of the laminar burning velocities of the premixed cyclopentanone-, gasoline- and ethanol-air mixtures using various equivalence ratios (initial condition: T_0=423K and P_0=0.1MPa). The trends of the differences were similar to those of the unstretched flame propagation speed, i.e. the larger differences occurred with richer mixtures. This is in agreement with Ref [25]. The laminar burning velocity of the cyclopentanone-air mixture was similar to that of ethanol-air mixtures when ϕ was less than 1.0. However, when the mixture was richer (ϕ>1.0), the laminar burning velocities of the cyclopentanone-air mixtures were lower than those of the ethanol-air mixtures at the same equivalence ratios, and the difference between the two fuels increased when the equivalence ratio was increased. Compared with the gasoline-air mixtures, the laminar burning velocity of the cyclopentanone-air mixtures was consistently higher when ϕ is higher than 1.0; when ϕ was lower than 1.0, the difference in the laminar burning velocities between cyclopentanone-air and gasoline-air mixtures was smaller. At an initial condition of T_0=423K and P_0=0.1MPa, the maximum laminar burning velocity of cyclopentanone was 0.82m/s, whereas for gasoline, it was 0.72m/s, and for ethanol, it was 0.86m/s.

3.4 Normalization and empirical correlation

Generally, laminar burning velocity depends on initial mixture composition, pressure and temperature [13, 24]. For a given fuel-air mixture and a given initial pressure, the relationship between laminar burning velocity and initial temperature can be expressed using the following equation [50]:

$$\frac{\mathrm{u}_{\mathrm{l}}}{\mathrm{u}_{\mathrm{l0}}}=\left(\frac{T_0}{T_{\mathrm{u0}}}\right)^{\alpha_T} \qquad （8）$$

where u_{l0} is the reference laminar burning velocity at the initial reference temperature of T_{u0} and α_T is the temperature exponent.

Given this relationship, it is believed that it is possible to obtain laminar burning velocities for a certain fuel at varied initial temperatures if the temperature exponent α_T and the reference laminar burning speed u_{l0}, at the initial reference temperature of T_{u0}, are known. Figure 12 shows the fitting result of the reference laminar burning velocity u_{l0} (initial condition: T_{u0}=423K and P_0=0.1MPa) and the temperature exponent α_T (calculated using the data from Figure 11a for cyclopentanone). Their fitting formulas are obtained from the test data presented above, and they are as follows.

$$u_{l0}=-0.8666\phi^4+4.3589\phi^3-9.6216\phi^2+10.17\phi-3.2687 \qquad （9）$$

$$\alpha_T=6.4441\phi^3-20.379\phi^2+21.215\phi-5.6018 \qquad （10）$$

From Equations 8-10, the laminar burning velocity of cyclopentanone can be calculated using Equation 11:

$$u_l=(-0.8666\phi^4+4.3589\phi^3-9.6216\phi^2+10.17\phi-3.2687)\left(\frac{T_0}{423}\right)^{6.4441\phi^3-20.379\phi^2+21.215\phi-5.6018} \qquad (11)$$

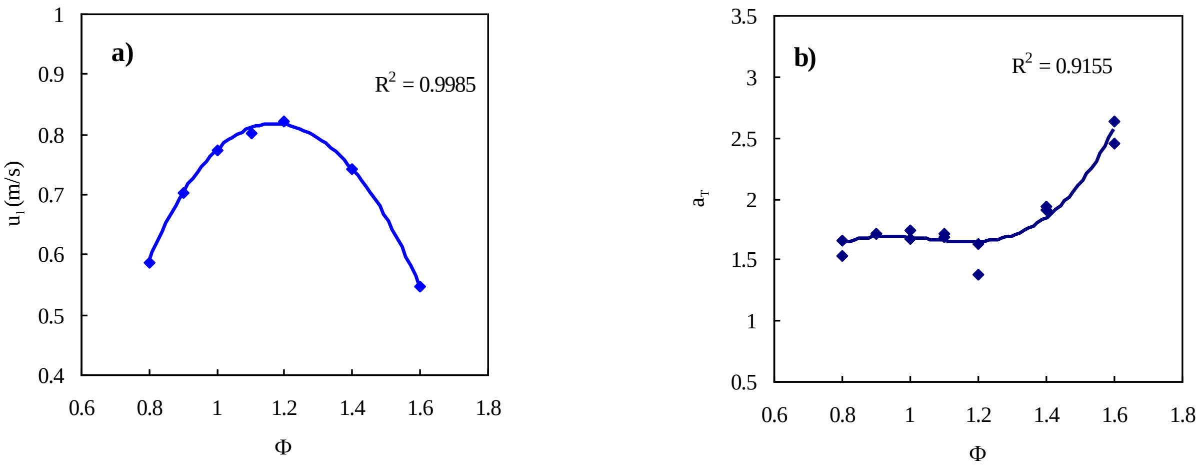

Figure 12 Reference laminar burning velocity and temperature exponent (initial condition: P_0=0.1MPa)

(a) reference laminar burning velocity; (b) temperature exponent

Figure 13 shows the comparison of the experimental data and the correlation predictions data, calculated from the empirical fitting Equation 11. It can be seen that the calculated data using Equation 11 matched well with the experimental data. The deviations of these two kinds of data were less than 0.02m/s, i.e., within an error of 4%.

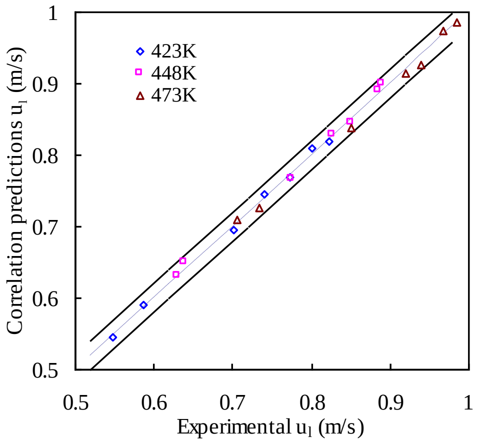

Figure 13 Comparison of correlation predictions and experimental data (initial condition: P_0=0.1MPa)

4 Conclusions

Laminar flame combustion characteristics of premixed cyclopentanone-air mixtures at elevated temperatures have been investigated in a constant-volume vessel using the high-speed Schlieren photography technique, and compared with gasoline and ethanol. The main conclusions drawn from the study are as follows:

1) The Markstein length of cyclopentanone laminar flame does not appear to change with initial temperature and it decreases when equivalence ratio is increased. Its sensitivity to equivalence ratio is higher than that of ethanol and lower than that of gasoline, although the trend is similar to them. The turning point of equivalence ratio at which it changes from positive to negative is slightly below1.4.
2) The maximum laminar burning velocity of cyclopentanone occurs at the equivalence ratio of 1.2, regardless of the initial temperature. The corresponding equivalence ratio is slightly leaner than for gasoline (1.1 to 1.2) but richer than for ethanol (1.2 and 1.3).
3) When the equivalence ratio is leaner than stoichiometric, the laminar burning velocity of cyclopentanone has smaller differences to that of ethanol and gasoline. When the equivalence ratio increases, it becomes increasingly lower than that of ethanol and higher than that of gasoline.
4) At an initial temperature of 423K and initial pressure of 0.1MPa, the maximum laminar burning velocity of the cyclopentanone is 0.82 m/s, for gasoline it is 0.72 m/s and for ethanol it is 0.86m/s.

Acknowledgement

This work is supported by the State Key Laboratory of Engines at Tianjin University (K2016-03), the Chinese Ministry of Education (Z2015084) , Xihua University (11ZA283, Z1120318), the Science & Technology Department of Sichuan Province (2016ZR0047), and EPSRC(EP/N021746/1).

References

[1] Wu X, Li Q, Fu J, Tang C, Huang Z, Daniel R, et al. Laminar burning characteristics of 2,5-dimethylfuran and iso-octane blend at elevated temperatures and pressures. Fuel 2012;95:234–40.

[2] Agarwal AK. Biofuels (alcohols and biodiesel) applications as fuels for internal combustion engines. Prog Energy Combust Sci 2007;33:233–71.

[3] Strobel GA, Knighton B, Kluck K, Ren Y, Livinghouse T, Griffin M, et al. The production of myco-diesel hydrocarbons and their derivatives by the endophytic fungus Gliocladium roseum (NRRL 50072). Microbiology 2008;154:3319–28.

[4] Demirbas A. Progress and recent trends in biofuels. Prog Energy Combust Sci 2007;33:1–18.

[5] Singh SK, Strobel GA, Knighton B, Geary B, Sears J, Ezra D. An endophytic Phomopsis sp. Possessing bioactivity and fuel

potential with its volatile organic compounds. Microbial Ecology 2011;61(4):729–39.

[6] Román-Leshkov Y, Barrett CJ, Liu ZY, Dumesic JA. Production of dimethylfuran for liquid fuels from biomass-derived carbohydrates. Nature 2007;447:982–5.

[7] Zhao H, Holladay JE, Brown H, Zhang ZC. Metal chlorides in ionic liquid solvents convert sugars to 5-hydroxymethylfurfural. Science 2007;316: 1597–600.

[8] Anbarasan P, Baer ZC, Sreekumar S, Gross E, Binder JB, Blanch HW, et al. Integration of chemical catalysis with extractive fermentation to produce fuels. Nature 2012;491:235–9.

[9] Allen JW, Scheer AM, Gao CW, Merchant SS, Vasu SS, Welz O, et al. A coordinated investigation of the combustion chemistry of diisopropyl ketone, a prototype for biofuels produced by endophytic fungi. Combust Flame 2014;161:711–24.

[10] Serinyel Z, Togbé C, Zaras A, Dayma G, Dagaut P. Kinetics of oxidation of cyclohexanone in a jet-stirred reactor: Experimental and modeling. Proceedings of the Combustion Institute 2015;35(1):507–14.

[11] Yang J, Li N, Li G, Wang W, Wang A, Wang X, et al. Synthesis of renewable high-density fuels using cyclopentanone derived from lignocellulose. Chem Commun 2014;50:2572–4.

[12] Elliott DC, Hart TR. Catalytic hydroprocessing of chemical models for bio-oil. Energy Fuels 2009;23(2):631–7.

[13] Heywood J. Internal combustion engine fundamentals. Mcraw-Hill Inc.; 1988.

[14] Christensen E, Yanowitz J, Ratcliff M, McCormick RL. Renewable oxygenate blending effects on gasoline properties. Energy Fuels 2011;25:4723–33.

[15] Yanowitz J, Christensen E, McCormick RL. Utilization of renewable oxygenates as gasoline blending components. Contract 2011;303:275–3000.

[16] Gas L. Lower and upper explosive limits for flammable gases and vapors (LEL/UEL). Matheson gas products 2013;22.

[17] Knovel. Knovel Critical Tables (2nd Edition), https://app.knovel.com/web/index.v/; 2008 [accessed 16.11.10].

[18] Metghalchi M, Keck JC. Laminar burning velocity of propane–air mixtures at high temperature and pressure. Combust Flame 1980;38:143–54.

[19] Law CK, Sung CJ, Wang H, Lu TF. Development of comprehensive detailed and reduced reaction mechanisms for combustion modeling. AIAA J 2003;41:1629–46.

[20] Lewis B, Elbe G. Combustion, flames and explosions of gases. New York: Academic Press; 1987.

[21] Levy A, Weinberg FJ. Optical flame structure studies: Some conclusions concerning the propagation of flat flames. Symposium (International) on Combustion 1958;7(1):296–303.

[22] Egolfopoulos FNN, Cho P, Law CKK. Laminar flame speeds of methane-air mixtures under reduced and elevated pressures. Combust Flame 1989;76(3–4):375–91.

[23] Huang Y, Sung CJ, Eng JA. Laminar flame speeds of primary reference fuels and reformer gas mixtures. Combustion and Flame 2004;139:239–51.

[24] Egolfopoulos FN, Hansen N, Ju Y, Kohse-Höinghaus K, Law CK, Qi F. Advances and challenges in laminar flame experiments and implications for combustion chemistry. Progress in Energy and Combustion Science 2014;43:36–67.

[25] Tian G, Daniel R, Li H, Xu H, Shuai S, Richards P. Laminar burning velocities of 2,5-dimethylfuran compared with ethanol and gasoline. Energy Fuels 2010;27(7):3898–905.

[26] Ma X, Jiang C, Xu H, Ding H, Shuai S. Laminar burning characteristics of 2-methylfuran and isooctane blend fuels. Fuel 2014;116:281–91.

[27] Ma X, Jiang C, Xu H, Shuai S, Ding H. Laminar burning characteristics of 2-methylfuran compared with 2,5-dimethylfuran and isooctane. Energy & Fuels 2013;27(10):6212–21.

[28] Badawy T, Williamson J, Xu H. Laminar burning characteristics of ethyl propionate, ethyl butyrate, ethyl acetate, gasoline and ethanol fuels. Fuel 2016;183:627–40.

[29] Jiang Y, Xu H, Ma X, Bao X, Wang B. Laminar burning characteristics of 2-MTHF compared with ethanol and isooctane. Fuel 2017;190:10–20.

[30] Bao X, Combustion characteristics of premixed hydrogen-air mixtures in a constant volume vessel, PhD thesis, Beijing Institute of Technology, 2011.

[31] Liu F, Bao X, Gu J, Chen R. Onset of cellular instabilities in spherically propagating hydrogen-air premixed laminar flames. International Journal of Hydrogen Energy 2012;37:11458–65.

[32] Zaras AM, Dagaut P, Serinyel Z. Computational kinetic study for the unimolecular decomposition pathways of cyclohexanone. The Journal of Physical Chemistry A 2014;119(28):7138–44.

[33] Bradley D, Gaskell PH, Gu XJ. Burning velocities, markstein lengths, and flame quenching for spherical methane-air flames: a computational study. Combust Flame 1996;104:176–98.

[34] Clavin P. Dynamic behaviour of premixed flame fronts in laminar and turbulent flows. Prog Energy Combust Sci 1985;11:1–59.

[35] Bradley D, Hicks R, Lawes M, Sheppard CG, Wooley R. The measurement of laminar burning velocities and Markstein numbers for iso-octane–air and isooctane–n-heptane–air mixtures at elevated temperatures and pressures in an explosion bomb. Combust Flame 1998;115(1–2):126–44.

[36] Frankel ML, Sivashinsky GI. On effects due to thermal expansion and Lewis number in spherical flame propagation. Combustion Science and Technology 1983;31:131–8.

[37] Kelley AP, Jomaas G, Law CK. Critical radius for sustained propagation of spark-ignited spherical flames. Combust Flame 2009;156:1006–13.

[38] Chen Z. On the extraction of laminar flame speed and Markstein length from outwardly propagating spherical flames. Combust Flame 2011;158:291–300.

[39] Shen X, Yang X, Santner J, Sun J, Ju Y. Experimental and kinetic studies of acetylene flames at elevated pressures. Proceedings of the Combustion Institute 2015;35:721–8.

[40] Wu F, Liang W, Chen Z, Ju Y, Law CK. Proceedings of the Combustion Institute 2015;35:663–70.

[41] Morley C. GASEQ: A chemical equilibrium program for Windows, http://www.gaseq.co.uk/; 2005 [accessed 16.11.10].

[42] Eisazadeh-Far K, Parsinejad F, Metghalchi H, Keck JC. On flame kernel formation and propagation in premixed gases. Combustion and Flame 2010;157:2211–21.

[43] Moghaddas A, Eisazadeh-Far K, Metghalchi H. Laminar burning speed measurement of premixed n-decane/air mixtures using spherically expanding flames at high temperatures and pressures. Combustion and Flame 2012;159:1437–43.

[44] Egolfopoulos FN, Du DX, Law CK. A study on ethanol oxidation kinetics in laminar premixed flames, flow reactors, and shock tubes. Symposium (international) on combustion 1992;24(1):833–41.

[45] Eisazadeh-Far K, Moghaddas A, Al-Mulki J, Metghalchi H. Laminar burning speeds of ethanol/air/diluent mixtures. Proceedings of the Combustion Institute 2011;33:1021–7.

[46] Bradley D, Lawes M, Mansour MS. Explosion bomb measurements of ethanol–air laminar gaseous flame characteristics at pressures up to 1.4 MPa. Combustion and Flame 2009;156:1462–70.

[47] Tawfik Badawy T, Bao X, Xu H. Impact of spark plug gap on flame kernel propagation and engine performance. Applied Energy, Volume 191, 1 April 2017, Pages 311–327

[48] Matalon M. Flame dynamics. Proc Combust Inst 2009;32:57–82.

[49] Gu XL, Huang ZH, Wu S, Li QQ. Laminar burning velocities and flame instabilities of butanol isomers–air mixtures. Combust Flame 2010;157:2318–25.

[50] Glassman I, Yetter RA. Combustion. 4th ed. Amsterdam, Boston: Academic Press; 2008.